1521-0111/89/1/133–140$25.00
MOLECULAR PHARMACOLOGY

http://dx.doi.org/10.1124/mol.115.101618
Mol Pharmacol 89:133–140, January 2016

Bumetanide Derivatives AqB007 and AqB011 Selectively Block the Aquaporin-1 Ion Channel Conductance and Slow Cancer Cell Migration

Mohamad Kourghi,[1] Jinxin V. Pei,[1] Michael L. De Ieso, Gary Flynn, and Andrea J. Yool

School of Medicine (M.K., J.V.P., M.L.D.I., A.J.Y.) and Institute for Photonics and Advanced Sensing (J.V.P., A.J.Y.), University of Adelaide, Adelaide, South Australia, Australia; and Spacefill Enterprises LLC, Oro Valley, Arizona (G.F.)

Received September 3, 2015; accepted October 13, 2015

ABSTRACT

Aquaporins (AQPs) in the major intrinsic family of proteins mediate fluxes of water and other small solutes across cell membranes. AQP1 is a water channel, and under permissive conditions, a nonselective cation channel gated by cGMP. In addition to mediating fluid transport, AQP1 expression facilitates rapid cell migration in cell types including colon cancers and glioblastoma. Work here defines new pharmacological derivatives of bumetanide that selectively inhibit the ion channel, but not the water channel, activity of AQP1. Human AQP1 was analyzed in the *Xenopus laevis* oocyte expression system by two-electrode voltage clamp and optical osmotic swelling assays. The aquaporin ligand bumetanide derivative AqB011 was the most potent blocker of the AQP1 ion conductance (IC_{50} of 14 μM), with no effect on water channel activity (at up to 200 μM). The order of potency for inhibition of the ionic conductance was AqB011 > AqB007 >> AqB006 ≥ AqB001. Migration of human colon cancer (HT29) cells was assessed with a wound-closure assay in the presence of a mitotic inhibitor. AqB011 and AqB007 significantly reduced migration rates of AQP1-positive HT29 cells without affecting viability. The order of potency for AQP1 ion channel block matched the order for inhibition of cell migration, as well as in silico modeling of the predicted order of energetically favored binding. Docking models suggest that AqB011 and AqB007 interact with the intracellular loop D domain, a region involved in AQP channel gating. Inhibition of AQP1 ionic conductance could be a useful adjunct therapeutic approach for reducing metastasis in cancers that upregulate AQP1 expression.

Introduction

Osmotic water transport across biologic membranes is facilitated by membrane proteins known as aquaporins (AQPs), which are found in all kingdoms of life (Reizer et al., 1993; Park and Saier, 1996; Campbell et al., 2008). To date, at least 15 mammalian subfamilies have been identified: AQP0–AQP14 (Ishibashi, 2009; Finn et al., 2014). Aquaporin is organized as a tetramer of subunits, each comprising six transmembrane domains and five loops (A–E) and carrying a monomeric pore that allows the movement of water or other small solutes (Jung et al., 1994; Fu et al., 2000; Sui et al., 2001).

There is increasing recognition that certain classes of aggressive cancers depend on upregulation of AQP1 for fast migration and metastasis (Monzani et al., 2007). Although the precise mechanism for AQP1-enhanced motility remains unknown, both ion and water channels are essential in the cellular migration process (Schwab et al., 2007). AQP1 expression has been linked to metastasis and invasiveness of colon cancer cells (Jiang, 2009; Yoshida et al., 2013). In mammary and melanoma cancer cells, AQP1 facilitates tumor cell migration in vitro and metastasis in vivo (Hu and Verkman, 2006). Increased levels of AQP1 expression in astrocytoma correlate with the clinical grade, serving as a diagnostic indicator of poor prognoses (El Hindy et al., 2013). AQP1-facilitated cell migration in glioma cannot be substituted by AQP4, indicating more than a simple water channel function is involved in the migration-enhancing mechanism (McCoy and Sontheimer, 2007).

A subset of aquaporins have been shown to have ion channel function, including AQP0, AQP1, AQP6, plant nodulin, and *Drosophila* big brain (Yool and Campbell, 2012). In AQP1, multiple lines of evidence have shown the cGMP-dependent monovalent cation channel is located in the central pore at the 4-fold axis of symmetry and is pharmacologically distinct from the monomeric water pores (Anthony et al., 2000; Saparov et al., 2001; Boassa and Yool, 2003; Yu et al., 2006; Zhang et al., 2007). The AQP1 ion channel has a unitary conductance of 150 picosiemens in physiologic saline, slow activation and deactivation kinetics, and is permeable to Na^+, K^+, and Cs^+, but not divalent cations (Yool et al., 1996; Anthony et al., 2000). Loop D has been shown previously to be involved in cGMP-dependent gating of AQP1 ion channels (Yu et al.,

This work was supported in part by the National Institutes of Health [Grant R01 GM059986] and a 2015 pilot grant from the Institute for Photonics and Advanced Sensing, University of Adelaide.
[1]M.K. and J.V.P. are co-first authors.
dx.doi.org/10.1124/mol.115.101618.
This article has supplemental material available at molpharm.aspetjournals.org.

ABBREVIATIONS: AqB, aquaporin ligand bumetanide derivative (in numbered series); AQP1, aquaporin-1; DMSO, dimethylsulfoxide; EtOAC, ethyl acetate; MW, molecular weight.

2006). The low proportion of AQP1 water channels that are available to be gated as ion channels in reconstituted bilayers and heterologous expression systems has prompted uncertainty regarding the physiologic relevance of the dual water and ion channel function in AQP1 (Saparov et al., 2001; Tsunoda et al., 2004). Further work has indicated that the availability of AQP1 ion channels to be activated by cGMP depends in part on tyrosine phosphorylation at the carboxyl terminal domain (Campbell et al., 2012).

Our characterization here of selective nontoxic pharmacological blockers of the AQP1 ion channel opens the first opportunity to define the functional roles of the AQP1 ion conductance. Prior to 2009, available AQP1 blockers were limited by low potency, lack of specificity, or toxicity. Mercury potently blocks AQP1 water permeability by covalent modification of a cysteine residue in loop E (Preston et al., 1993), but is highly toxic. The tetrethylammonium ion blocks the AQP1 water pore, although not in all cell types (Brooks et al., 2000; Detmers et al., 2006; Sogaard and Zeuthen, 2008), and the cadmium ion blocks the AQP1 ion channel (Boassa et al., 2006), but both lack selectivity for aquaporins. Effective compounds discovered recently include the arylsulfonamides AqB013, which blocks AQP1 and AQP4 water channel permeability (Migliati et al., 2009), and AqF026, which strongly potentiates AQP1 water channel activity (Yool et al., 2013). Other arylsulfonamides have been proposed as blockers of AQP4 channels (Huber et al., 2009). A distinct class of agents acting on the external side of the membrane to block human AQP1 water flux has been identified as a source of candidate lead compounds for drug development (Seeliger et al., 2013).

Work here characterizes a novel set of aquaporin ligand bumetanide derivative (AqB) compounds that differentially block the AQP1 ion channel without affecting water permeability. The most potent of these, AqB011, is a promising tool for dissecting the role of the AQP1 ion channel while sparing osmotic water permeability. Understanding the functional roles and regulation of AQP1 is essential for determining the full range of physiologic roles it might serve and its possible value as a therapeutic target in cancer metastasis.

Materials and Methods

Oocyte Preparation and Injection. The use of animals in this study has been carried out in accordance with the Guide for the Care and Use of Laboratory Animals, licensed under the South Australian Animal Welfare Act 1985, with protocols approved by the University of Adelaide Animal Ethics Committee. Unfertilized oocytes were harvested from anesthetized *Xenopus laevis* frogs and defoliculated by incubation in type 1A collagenase (2 mg/ml) with a trypsin inhibitor (0.3 mg/ml) in OR-2 saline (82 mM NaCl, 2.5 mM KCl, 1 mM $MgCl_2$, and 5 mM HEPES; pH 7.3) at 16–18°C for 2 to 3 hours. Human aquaporin-1 cDNA was provided by Professor P. Agre (Preston et al., 1992; GenBank accession number NM_198098). AQP1 subcloned into a *X. laevis* β-globin plasmid was linearized with BamHI and transcribed in vitro (T3 mMessage mMachine; Ambion Inc., Austin, TX), and cRNA was resuspended in sterile water. Prepared oocytes were injected with 50 nl of water (non–AQP1-expressing control oocytes) or 50 nl of water containing 1 ng of AQP1 cRNA and incubated for 2 or more days at 16°C in ND96 saline (96 mM NaCl, 2 mM KCl, 1 mM $MgCl_2$, 1.8 mM $CaCl_2$, and 5 mM HEPES, pH 7.3) to allow protein expression. Successful expression was confirmed by osmotic swelling assays. Batches of AQP1-expressing oocytes that lacked robust cGMP-activated conductance responses were further incubated overnight in ND96 saline with the tyrosine phosphatase inhibitor bisperoxovanadium (100 μM; Santa Cruz Biotechnology, Dallas, TX) per published methods (Campbell et al., 2012). Chemicals were purchased from Sigma-Aldrich (St. Louis, MO) unless otherwise specified.

AqB Compounds: Synthesis and Preparation. The AqB compounds (custom-designed bumetanide derivatives) were synthesized by Dr. G. Flynn (Spacefill Enterprises LLC, Oro Valley, AZ) as described in U.S. patent 8,835,491-B2. To make AqB001, bumetanide was mixed with diazomethane (CH_2N_2) generated by reaction with Diazald to create bumetanide methyl ester [molecular weight (MW) 344.8; ClogP 2.10], which was dissolved in hot $CHCl_3$, diluted with hexanes and allowed to cool to provide the purified methyl ester as white flakes, whose mass and NMR spectra were consistent with the desired product. Reaction of bumetanide with 1.2 equivalents of 1,1′-carbonyldiimidazole in ethyl acetate (EtOAC) under argon with heating afforded an intermediate imidazolide, which upon cooling, formed a white solid that could be isolated by filtration and stored under argon for later use. Alternatively, the imidazolide solution could be reacted in situ with two equivalents of an amine to form the corresponding amides. In a typical reaction, the reaction mixture would be partitioned between water and EtOAC, the organic layer would be washed with brine, the solution would be filtered and concentrated, and the residue would be crystallized to form EtOAc/hexanes. AqB-006 (MW 413.9; ClogP 1.04) was prepared using morpholine as the amine; AqB007 (MW 470.0; ClogP 0.79) resulted from 2-(4-methylpiperazine-1-yl) ethylamine; and AqB011 (MW 434.9; ClogP 1.80) was prepared using 2-(morpholine-1-yl)ethylamine. The structures of all the compounds were confirmed by high-resolution mass spectrometry and NMR analysis. Chemicals were purchased from Sigma-Aldrich unless otherwise specified.

Powdered compounds were dissolved in dimethylsulfoxide (DMSO) to create 1000× stock solutions for each desired final dosage. An equal dilution of DMSO (0.1%) alone in saline was used as the vehicle control.

Quantitative Swelling Assay. For double-swelling assays, each oocyte served as its own control. Swelling rates were assayed first without drug treatment (S1), and then oocytes incubated for 2 hours in isotonic saline with or without the AqB compounds were reassessed in a second swelling assay (S2). Swelling rates in 50% hypotonic saline (isotonic Na saline diluted with an equal volume of water) were quantified by relative increases in the oocyte cross-sectional area imaged by videomicroscopy (charge-coupled device camera; Cohu, San Diego, CA) at 0.5 frames per second for 30 seconds using National Institutes of Health ImageJ software (Bethesda, MD). Rates were measured as the slopes of the linear regression fits of relative volume as a function of time using Prism (GraphPad Software Inc., San Diego, CA).

Electrophysiology. For the two-electrode voltage clamp, capillary glass electrodes (1–3 MΩ) were filled with 1 M KCl. Recordings were done in standard Na^+ bath saline containing 100 mM NaCl, 2 mM KCl, 4.5 mM $MgCl_2$, and 5 mM HEPES, pH 7.3. cGMP was applied extracellularly at a final concentration of 10–20 μM using the membrane-permeable cGMP analog (Rp)-8-(*para*-chlorophenylthio)-cGMP. Ionic conductance was monitored for at least 20 minutes after cGMP addition to allow development of maximal plateau responses. Conductance was determined by voltage step protocols from +60 to −110 mV from a holding potential of −40 mV. Recordings were made with a GeneClamp amplifier and pClamp 9.0 software (Molecular Devices, Sunnyvale, CA).

Circular Wound Closure Assay. The cancer cell lines used in this study were HT29 human colorectal adenocarcinoma cells (Chen et al., 1987) purchased from American Type Culture Collection (HTB-38; Manassas, VA), which strongly express endogenous AQP1, and SW480 human colorectal adenocarcinoma cells (CCL-228; from American Type Culture Collection), which express AQP5 but show little AQP1 expression. mRNA levels were evaluated by quantitative polymerase chain reaction and protein levels by western blot (H. Dorward et al., submitted manuscript). Confluent cultures of

HT29 and SW480 cells were used in migration assays to measure the effects of AqB treatments on rates of wound closure. Cells were plated in flat-bottom 96-well plates at 1.25×10^5 cells/well in Dulbecco's modified Eagle's medium with 10% fetal bovine serum and incubated at 37°C and 5% CO_2 for 12–18 hours to allow monolayer formation. Circular wounds were created by aspirating a central circle of cells with a p10 pipette. Wells were washed 2 to 3 times with phosphate-buffered saline to remove cell debris. Culture media (Dulbecco's modified Eagle's medium with 2% bovine calf serum) containing either vehicle or drug treatments in the presence of a mitotic inhibitor 5-fluoro-2′-deoxyuridine (100 ng/ml) were administered into the wells. Cultures were imaged at 0 and 24 hours and analyzed using ImageJ software to calculate the percent wound closure by the change in area:

$$[(\text{Area}_0 - \text{Area}_{24})/\text{Area}_0] \times 100$$

Cytotoxicity Assay. Cell viability was quantified using the alamarBlue cell viability assay (Molecular Probes, Eugene, OR). Cells were plated at 10^4 cells/well in 96-well plates, and fluorescence signal levels were measured with a FLUOstar Optima microplate reader (BMG Labtech, Victoria, Australia) after 24-hour incubation, with concentrations of AqB011 ranging from 1 to 80 μM, to obtain quantitative measures of cell viability. Mercuric chloride (20 μM) was used as a positive control for cytotoxicity.

Molecular Modeling. In silico modeling was conducted with methods reported previously (Yool et al., 2013). The crystal structure of human AQP1 was obtained from the Protein Data Bank (PDB) (identity 1FQY). The tetrameric model (Supplemental Material) was generated in Pymol (Version 1.7.4; Schrödinger, LLC; Mannheim, Germany) using coordinates provided in the pdb file. Renderings of the AqB ligands were generated in Chemdraw (Version 13.0; PerkinElmer, MA) and then converted into the pdb format using the online SMILES translation tool (National Cancer Institute, U.S. Department Health and Human Services, Washington, DC). Both AQP1 and ligand coordinates were prepared for docking using MGLtools (Version 1.5.4; Scripps Institute, San Diego, CA). The docking was carried using Autodock Vina (Trott and Olson, 2010), with a docking grid covering the intracellular face of tetrameric pore.

Data Compilation and Statistics. The results compiled from replicate experiments are presented as box plots. The boxes represent 50% of the data, the error bars indicate the full range, and the horizontal bars are the median values. The n values are in italics above the x-axis. Statistical differences were analyzed with one-way analysis of variance and post hoc Bonferroni tests and reported as $^{**}P < 0.0001$, $^{*}P < 0.05$, and N.S. ($P > 0.05$).

Results

AQP1 Ion Channel Inhibition by Novel Bumetanide Derivatives. A set of four related compounds with structural modifications at the carboxylic acid moiety of bumetanide was tested for effects on the cGMP-activated ionic conductance in AQP1-expressing oocytes. Two-electrode voltage clamp recordings of AQP1-expressing oocytes (Fig. 1) illustrate the inhibition of the ionic conductance by extracellular application of AqB007 (200 μM) and AqB011 (20 μM), but no appreciable block of the AQP1 ion channel with 200 μM AqB001 or AqB006. Initial recordings before cGMP application and responses to the first application of cGMP recordings showed typical cGMP-dependent activation, as described previously (Anthony et al., 2000). Oocytes were then transferred into saline with the indicated agents for 2 hours, during which time the ionic conductances uniformly recovered to initial levels (Fig. 2). In response to the second application of cGMP, oocytes treated with vehicle (DMSO), AqB001, or AqB006 showed increases in conductance that were comparable to the first response. However, the cGMP-activated conductance responses were inhibited after treatment with AqB007 or AqB011.

Trend plots (Fig. 2A) show that the ionic conductance in AQP1-expressing oocytes was initially low and activated by the first bath application of membrane-permeable cGMP. The ionic conductance then recovered to the basal level during 2-hour incubation without cGMP and was tested for reactivation by a second application of cGMP after treatment with vehicle or AqB compounds. Recordings for oocytes incubated in saline without DMSO during the recovery period were comparable to

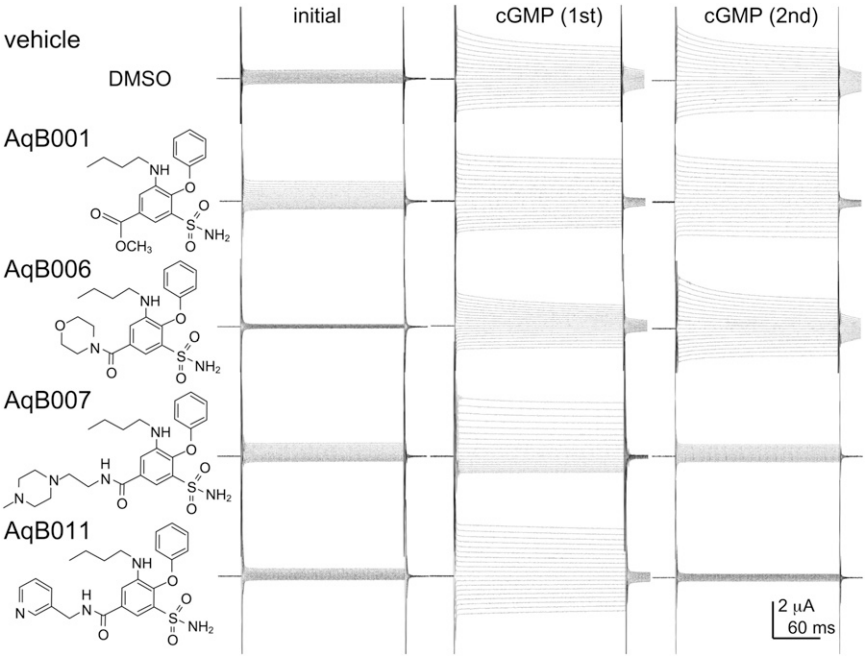

Fig. 1. Chemical structures of selected bumetanide derivatives and electrophysiology traces showing representative effects of AqB001, AqB006, AqB007, and AqB011 on the ionic conductance responses activated by bath application of CPT-cGMP before and after 2-hour incubation in saline with and without the AqB compounds. See *Materials and Methods* for details.

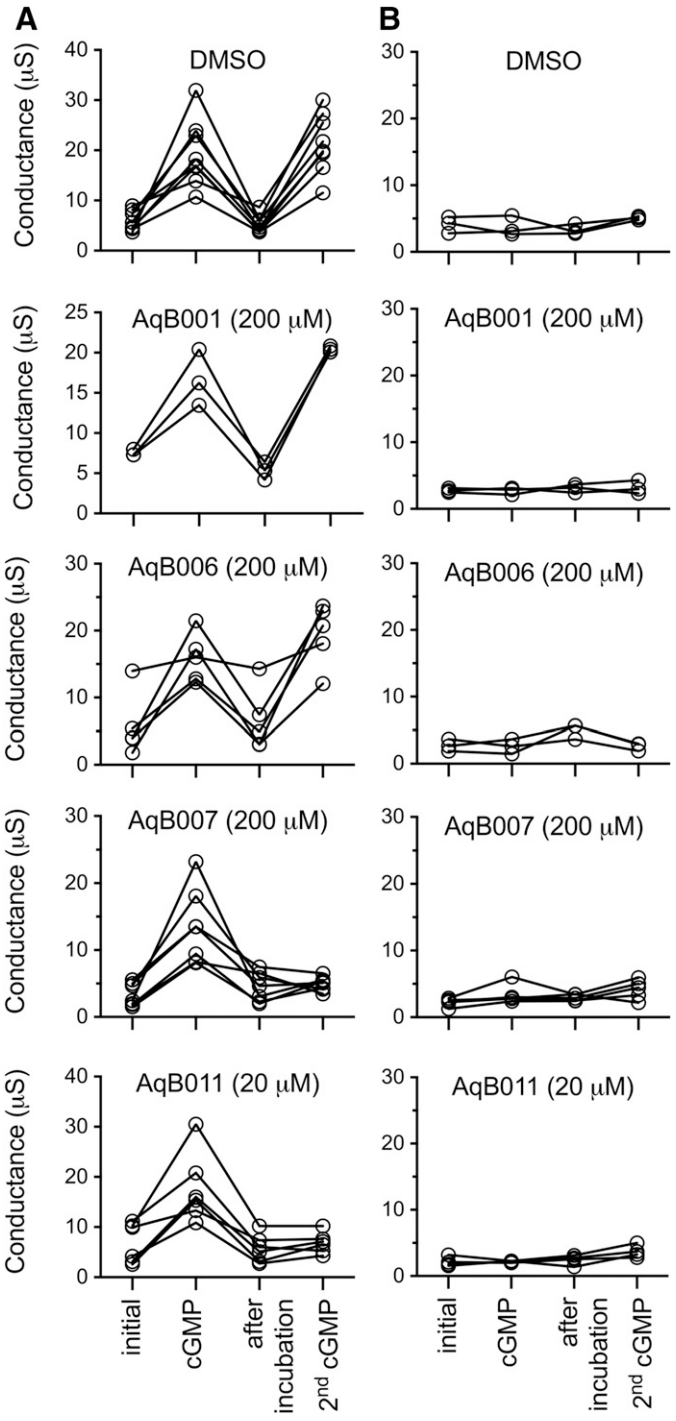

Fig. 2. Trend plots showing the ionic conductance responses for individual oocytes measured prior to cGMP (initial), after the first cGMP application, after 2-hour incubation in saline without cGMP containing DMSO (vehicle) or AqB agents, and after the second application of cGMP. Reversible cGMP-dependent activation of an ionic conductance in AQP1-expressing oocytes (A) was not seen in non-AQP1 control oocytes (B). Inhibition was seen after treatment with AqB007 and AqB011, but not with vehicle, AqB001, or AqB006.

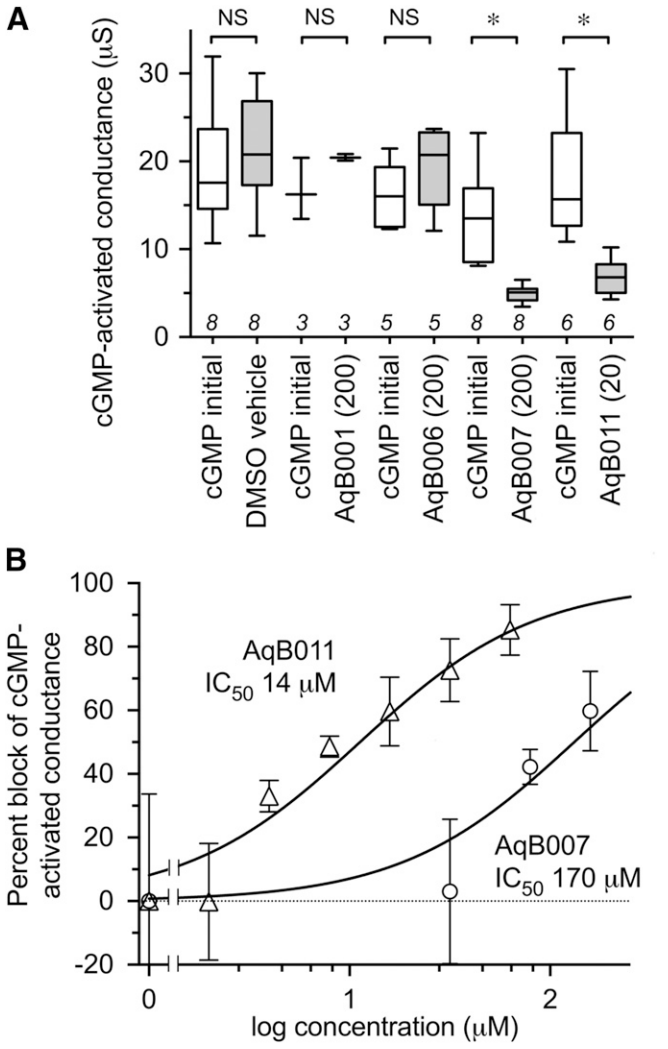

Fig. 3. Dose-dependent block of the AQP1 ionic conductance. (A) Compiled box plot data showing a statistically significant block of the cGMP-activated ionic conductance in AQP1-expressing oocytes by AqB007 and AqB011, but not with vehicle, AqB001, or AqB006. See *Materials and Methods* for details. (B) Dose-response curves showing percent block of the activated ionic conductance in AQP1-expressing oocytes and estimated IC_{50} values. *n* values for dose-response data (in order of increasing concentration) for AqB007 and AqB011 were 8, 4, 2, 8 and 8, 2, 2, 3, 6, 4, 3, respectively.

those for the DMSO-treated group (not shown). Non–AQP1-expressing control oocytes showed no ionic conductance response to cGMP and no effect of the vehicle or drug treatments (Fig. 2B).

Compiled data for the cGMP-activated ionic conductance values in AQP1-expressing oocytes are shown in the box plot (Fig. 3A) and indicate the levels of block by 200 μM AqB007 and 20 μM AqB011 were statistically significant as compared with initial responses to cGMP prior to treatment. Dose-response relationships (Fig. 3B) yielded estimated IC_{50} values of 14 μM for AqB011 and 170 μM for AqB007.

AqB Ion Channel Blockers Have No Effect on Osmotic Water Permeability. Data for oocyte volumes that were standardized as a percentage of the initial volume at time zero illustrate the mean swelling responses over 60 seconds after introduction of the oocytes into 50% hypotonic saline (Fig. 4A). AQP1-expressing oocytes showed consistent osmotic swelling, which was unaffected by treatment with vehicle (DMSO 0.1%) or AqB compounds at 200 μM each. Non–AQP1-expressing control oocytes showed little osmotic water permeability.

To analyze the possible effects of the AqB compounds on water channel activity, a double-swelling assay was used (Fig. 4B).

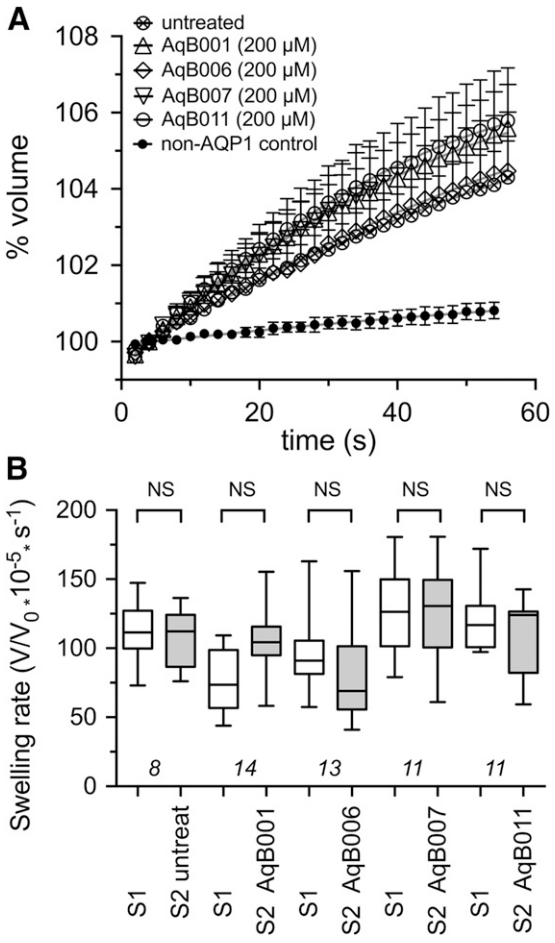

Fig. 4. Lack of effect of AqB compounds on AQP1 osmotic water permeability measured by optical swelling assays. (A) Mean oocyte volume, standardized as a percentage of the initial volume for each oocyte, as a function of time after introduction into 50% hypotonic saline, with and without 2-hour pretreatment with AqB compounds at 200 μM or vehicle (0.1% DMSO). (B) Compiled box plot data showing the absence of any statistically significant differences between the first and second swelling rates measured before (S1) and after (S2) 2-hour incubations in saline alone or saline with 200 μM AqB compounds as indicated. See *Materials and Methods* for details.

After the first swelling (S1) in hypotonic saline, oocytes were incubated in isotonic saline with or without the AqB compounds (200 μM) for 2 hours before assessing the second swelling response (S2). There were no significant differences between the first and second swelling rates in any of the treatment groups, confirming that the AqB ion channel agents did not affect AQP1 osmotic water permeability.

Molecular Modeling of Candidate Intracellular Binding Sites. Putative binding sites on the AQP1 ion pore for AqB011 and AqB007 in the intracellular loop D domain can be suggested based on structural modeling and docking analyses (Fig. 5). In silico modeling suggested the sites for the most favorable energies of interaction for AqB007 and AqB011 were located at the intracellular face of the central pore (Fig. 5A). Interestingly, the model predicted hydrogen bonding between the uniquely elongated moieties of the two effective AqB ligands and the initial pairs of arginine residues in the highly conserved loop D motifs from two adjacent subunits (Fig. 5B). The same arginines (R159 and R160 in human AQP1) have been shown to be involved in

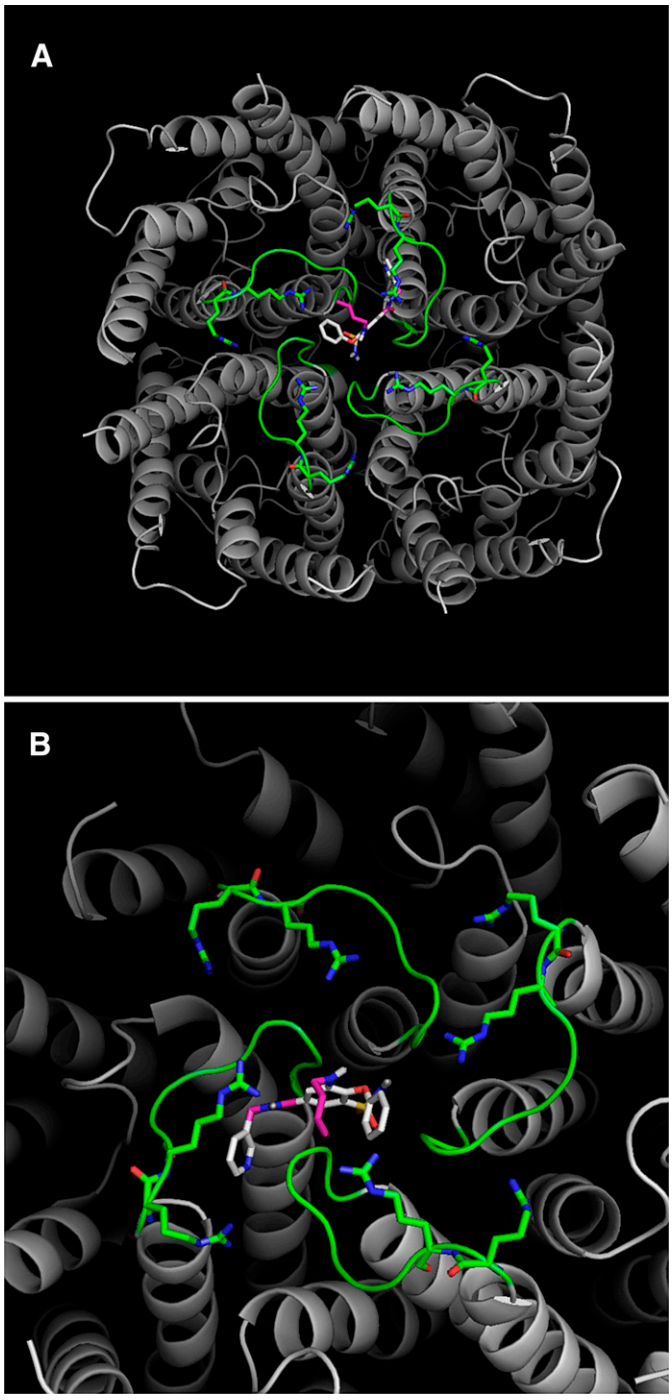

Fig. 5. In silico modeling of the energetically favored binding site for AqB011 in the center of the tetrameric channel of AQP1 (gray) at the intracellular side and bracketed by the gating loop D domains (green). The putative binding site suggests an interaction with two of the loop D domains from adjacent subunits. (A) is the full view of the tetramer, and (B) is a closer view slightly rotated to show proximity of the ligand to the conserved arginine residues in loop D.

AQP1 ion channel gating, but not water channel activity, in prior work (Yu et al., 2006). The more compact AqB006 docked weakly at a different position in the central vestibule (not shown). Although in silico modeling does not define actual binding sites, it provides a testable hypothesis for future work and offers intriguing support for the role of loop D in modulating AQP1 ion channel gating. The most

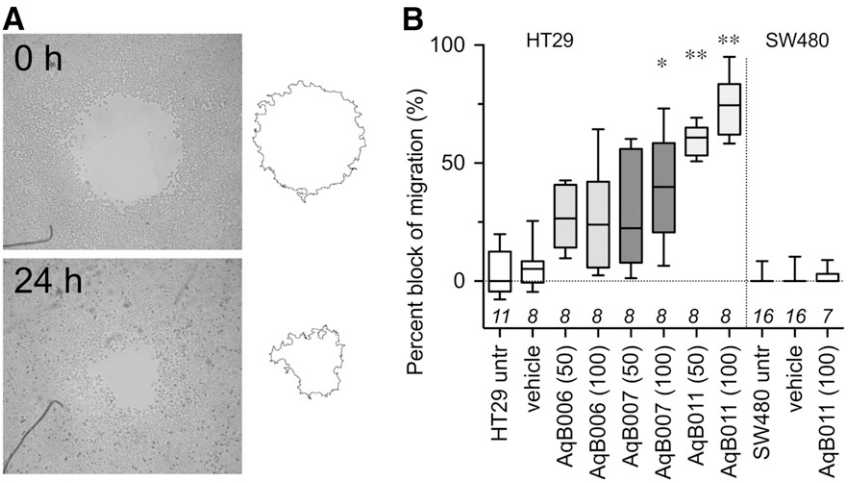

Fig. 6. Block of cell migration in AQP1-expressing HT29, but not SW480, cells treated with AqB011. (A) Illustrative diagram of the circular wound healing method showing substantial closure of the wounded area in normal culture medium by 24 hours. (B) Compiled box plot data from wound closure assays showing the dose-dependent inhibitory effects of AqB007 and AqB011 compared with DMSO and AqB006 on wound closure at 24 hours in HT29 cell cultures. Migration of SW480 cells was not altered by AqB011.

favorable energy of interaction was calculated for AqB011 (at −9.2 kcal/mol). The next most favorable energy of interaction for AqB compounds with the AQP1 channel was for AqB007 (at −7.0 kcal/mol), followed by AqB006 (at −6.0 kcal/mol). This order of interaction strength for the AqB series matched their order of efficacy for inhibition of the AQP1 ion channel conductance (Fig. 3).

Inhibition of AQP1 Ion Channel Activity Slows Cancer Cell Migration. The effects of AqB006, AqB007, and AqB011 were tested in migration assays of human HT29 colon cancer cells (Fig. 6), which natively express AQP1. Net migration rates were calculated from the percent closure of a circular wound area at 24 hours (Fig. 6A). The results showed that cancer cell migration was not impaired by AqB006, but was significantly impaired by AqB007 at 100 μM and AqB011 at 50 and 100 μM, as compared with vehicle-treated control HT29 cells (Fig. 6B). AqB011 was more effective than AqB007 in blocking migration, which is consistent with the relative efficacies of the agents as blockers of the ion channel conductance. In contrast, AqB011 at 100 μM had no effect on the migration rate of SW480 colon cancer cells (Fig. 6B), which express AQP5, but not AQP1, suggesting that the inhibitory effect of AqB011 appears to be selective for AQP1.

AqB Compounds Show Low Cytotoxicity. There was no significant difference in the viability of vehicle-treated and untreated cells and no effect of treatment with AqB011 for HT29 cells (Table 1). Cell viability was assessed with alamarBlue assays. The persistence of the fluorescent signal at 24 hours confirmed there was no appreciable cytotoxic effect of AqB011 treatment on HT29 cells at concentrations of up to 80 μM. Mercuric chloride as a positive control caused significant cell death, which was measured as a decrease in fluorescence. AqB011 at doses used to block the AQP1 ionic conductance and cancer cell migration did not impact cell viability.

Discussion

The aim of this study was to search for selective small-molecule pharmacological agents that are capable of blocking the cGMP-activated cationic conductance in AQP1. Discovery of pharmacological modulators for AQP1 channels has been an important goal in the aquaporin field. AQP1 antagonist and agonist agents are expected to be useful for defining the complex roles of aquaporins in fundamental biologic processes as well as characterizing AQP1 modulators as potential clinical agents in various conditions, such as cancer metastasis (Yool et al., 2010). AQP1 expression is upregulated in subtypes of aggressive cancer cells, in which it facilitates cancer migration. The results here show that selective blockers of the AQP1 ion channel slow the migration of human colon cancer cells in culture. Pharmacological inhibition of AQP1 is predicted to have a protective effect in reducing metastasis in cancer, but remains to be demonstrated in vivo.

Using bumetanide as a starting scaffold, we created an array of novel synthetic derivatives. Based on pilot data indicating a small inhibitory effect of AqB050 on the AQP1 ion channel at high doses (unpublished data), we investigated a series of structurally related derivatives, AqB006, AqB007, and AqB011, as well as a simple methylated version of bumetanide, AqB001, to test for possible inhibitors of the AQP1 ionic conductance. Our findings demonstrated that AqB007 and AqB011 are effective inhibitors of the central ion pore of AQP1, with estimated IC_{50} values of 170 and 14 μM, respectively. Both AqB007 and AqB011 showed dose-dependent inhibition of the central ion pore, whereas the intrasubunit water pores were unaffected, enabling the first dissection of physiologic roles of the distinct channel functions. Measuring fluorescence signal intensity with the alamarBlue

TABLE 1
HT29 cell levels of cytotoxicity after 24-hour incubation in culture medium with vehicle, AqB011, or $HgCl_2$

Agent (AqB011)	Mean Normalized Cell Viability ± S.E.M.[a]	*n* Value	Statistical Significance
μM	%		
0 (untreated)	100.0 ± 0.70	8	—
0 (0.1% DMSO)	103.9 ± 0.91	8	N.S.
1	104.0 ± 1.06	4	N.S.
5	102.3 ± 2.26	4	N.S.
10	110.6 ± 2.12	4	N.S.
20	114.0 ± 0.84	4	N.S.
40	111.8 ± 1.33	4	N.S.
80	102.4 ± 2.95	4	N.S.
$HgCl_2$ (100 μM)	16.2 ± 0.20	3	**

[a]Percent viability was standardized as a percentage of the untreated mean value measured as changes in alamarBlue fluorescence signal intensity. See *Materials and Methods* for details.

cell viability assay showed that AqB011 was not cytotoxic at doses that produced maximal ion channel inhibition.

The inhibition by AqB011 of AQP1 ionic conductance was consistent with molecular docking studies, suggesting the site of interaction is at the intracellular face of the central pore. The results revealed that AqB011 is the most energetically favored compound, followed by AqB007. The predicted interaction site of AqB011 and AqB007 with AQP1 is at the loop D domain. Differences in the structures and efficacies of AqB006, AqB007, and AqB011 indicate that the structure-activity relationship of ion channel inhibition is sensitive to specific chemical modifications at the carboxylic acid position of bumetanide. The length and structure of the modification appears to be critical and based on in silico modeling to be the region that interacts with the AQP1 channel gating loop D domain. The absence of cytotoxic effects of AqB011 at doses sufficient to block the AQP1 ion channel activity indicates that the inhibition of migration is not indirectly due to cell death. The observation that AqB011 inhibited migration in AQP1-expressing HT29 colon cancer cells, but had no effect on the migration of AQP-5–expressing SW480 colon cancer cells, provides support for the idea that AqB011 is selective for AQP1. The inhibition of migration seen with AqB011 is unlikely to result from off-target effects on general metabolic function, cytoskeletal organization, actin polymerization, or signaling pathways involved in cell motility since SW480 cell migration remained unaffected by the presence of AqB011.

AQP1 is present in barrier epithelia involved in fluid movement in the body, including the proximal tubule and choroid plexus (Agre et al., 1993). It is also expressed in peripheral microvasculature, dorsal root ganglion cells, eye ciliary epithelium and trabecular meshwork, heart ventricles, and other regions, in which a direct role for osmotic water flux is less evident (Yool, 2007). Additional roles suggested for AQP1 include angiogenesis (Nicchia et al., 2013), signal transduction (Oshio et al., 2006), increased mechanical compliance to changes in pressure (Baetz et al., 2009), axonal regeneration of spinal nerves (Zhang and Verkman, 2015), recovery from injury (Hara-Chikuma and Verkman, 2006), and exocytosis (Arnaoutova et al., 2008). Relative contributions of the ion and water channel functions in these diverse processes remain to be defined.

A possible role for the AQP1 ionic conductance (potentially in combination with water fluxes) in the control of cell volume associated with migration was supported by the results of the wound closure assays with AQP1-expressing HT29 cells. Cell migration was significantly impaired by AqB011 and AqB007, but not by AqB006. The greatest efficacy of migration block was seen with administration of AqB011. The comparable orders of efficacy for the block of AQP1 ion channels in the oocyte expression system and for the block of cell migration in HT29 cultures support the idea that the AqB011 effect on migration is mediated by direct block of the AQP1 ion channels. These data provide evidence that the ion channel activity of AQP1 has physiologic relevance. Further work is needed to evaluate the effects of blocking both water and ion channel activities of AQP1 together in migrating cells.

AqB011 is a new research tool for probing the physiologic role of the AQP1 ion channel function in biologic systems. This compound holds future promise as a possible adjunct clinical intervention in cancer metastasis. Exciting opportunities are likely to emerge from continuing discovery of pharmacological modulators for aquaporins for new treatments in cancers and other diseases.

Authorship Contributions

Participated in research design: Kourghi, Pei, De Ieso, Yool.
Conducted experiments: Kourghi, Pei, De Ieso.
Contributed new reagents or analytic tools: Flynn.
Performed data analysis: Kourghi, Pei, De Ieso, Yool.
Wrote or contributed to the writing of the manuscript: Kourghi, Pei, Flynn, Yool.

References

Agre P, Preston GM, Smith BL, Jung JS, Raina S, Moon C, Guggino WB, and Nielsen S (1993) Aquaporin CHIP: the archetypal molecular water channel. *Am J Physiol* **265**:F463–F476.

Anthony TL, Brooks HL, Boassa D, Leonov S, Yanochko GM, Regan JW, and Yool AJ (2000) Cloned human aquaporin-1 is a cyclic GMP-gated ion channel. *Mol Pharmacol* **57**:576–588.

Arnaoutova I, Cawley NX, Patel N, Kim T, Rathod T, and Loh YP (2008) Aquaporin 1 is important for maintaining secretory granule biogenesis in endocrine cells. *Mol Endocrinol* **22**:1924–1934.

Baetz NW, Hoffman EA, Yool AJ, and Stamer WD (2009) Role of aquaporin-1 in trabecular meshwork cell homeostasis during mechanical strain. *Exp Eye Res* **89**: 95–100.

Boassa D, Stamer WD, and Yool AJ (2006) Ion channel function of aquaporin-1 natively expressed in choroid plexus. *J Neurosci* **26**:7811–7819.

Boassa D and Yool AJ (2003) Single amino acids in the carboxyl terminal domain of aquaporin-1 contribute to cGMP-dependent ion channel activation. *BMC Physiol* **3**: 12.

Brooks HL, Regan JW, and Yool AJ (2000) Inhibition of aquaporin-1 water permeability by tetraethylammonium: involvement of the loop E pore region. *Mol Pharmacol* **57**:1021–1026.

Campbell EM, Ball A, Hoppler S, and Bowman AS (2008) Invertebrate aquaporins: a review. *J Comp Physiol B* **178**:935–955.

Campbell EM, Birdsell DN, and Yool AJ (2012) The activity of human aquaporin 1 as a cGMP-gated cation channel is regulated by tyrosine phosphorylation in the carboxyl-terminal domain. *Mol Pharmacol* **81**:97–105.

Chen TR, Drabkowski D, Hay RJ, Macy M, and Peterson W, Jr (1987) WiDr is a derivative of another colon adenocarcinoma cell line, HT-29. *Cancer Genet Cytogenet* **27**:125–134.

Detmers FJ, de Groot BL, Müller EM, Hinton A, Konings IB, Sze M, Flitsch SL, Grubmüller H, and Deen PM (2006) Quaternary ammonium compounds as water channel blockers. Specificity, potency, and site of action. *J Biol Chem* **281**: 14207–14214.

El Hindy N, Bankfalvi A, Herring A, Adamzik M, Lambertz N, Zhu Y, Siffert W, Sure U, and Sandalcioglu IE (2013) Correlation of aquaporin-1 water channel protein expression with tumor angiogenesis in human astrocytoma. *Anticancer Res* **33**: 609–613.

Finn RN, Chauvigné F, Hlidberg JB, Cutler CP, and Cerdà J (2014) The lineage-specific evolution of aquaporin gene clusters facilitated tetrapod terrestrial adaptation. *PLoS One* **9**:e113686.

Fu D, Libson A, Miercke LJ, Weitzman C, Nollert P, Krucinski J, and Stroud RM (2000) Structure of a glycerol-conducting channel and the basis for its selectivity. *Science* **290**:481–486.

Hara-Chikuma M and Verkman AS (2006) Aquaporin-1 facilitates epithelial cell migration in kidney proximal tubule. *J Am Soc Nephrol* **17**:39–45.

Hu J and Verkman AS (2006) Increased migration and metastatic potential of tumor cells expressing aquaporin water channels. *FASEB J* **20**:1892–1894.

Huber VJ, Tsujita M, and Nakada T (2009) Identification of aquaporin 4 inhibitors using in vitro and in silico methods. *Bioorg Med Chem* **17**:411–417.

Ishibashi K (2009) New members of mammalian aquaporins: AQP10-AQP12. *Handb Exp Pharmacol* 251–262.

Jiang Y (2009) Aquaporin-1 activity of plasma membrane affects HT20 colon cancer cell migration. *IUBMB Life* **61**:1001–1009.

Jung JS, Bhat RV, Preston GM, Guggino WB, Baraban JM, and Agre P (1994) Molecular characterization of an aquaporin cDNA from brain: candidate osmoreceptor and regulator of water balance. *Proc Natl Acad Sci USA* **91**:13052–13056.

McCoy E and Sontheimer H (2007) Expression and function of water channels (aquaporins) in migrating malignant astrocytes. *Glia* **55**:1034–1043.

Migliati E, Meurice N, DuBois P, Fang JS, Somasekharan S, Beckett E, Flynn G, and Yool AJ (2009) Inhibition of aquaporin-1 and aquaporin-4 water permeability by a derivative of the loop diuretic bumetanide acting at an internal pore-occluding binding site. *Mol Pharmacol* **76**:105–112.

Monzani E, Shtil AA, and La Porta CA (2007) The water channels, new druggable targets to combat cancer cell survival, invasiveness and metastasis. *Curr Drug Targets* **8**:1132–1137.

Nicchia GP, Stigliano C, Sparaneo A, Rossi A, Frigeri A, and Svelto M (2013) Inhibition of aquaporin-1 dependent angiogenesis impairs tumour growth in a mouse model of melanoma. *J Mol Med (Berl)* **91**:613–623.

Oshio K, Watanabe H, Yan D, Verkman AS, and Manley GT (2006) Impaired pain sensation in mice lacking aquaporin-1 water channels. *Biochem Biophys Res Commun* **341**:1022–1028.

Park JH and Saier MH, Jr (1996) Phylogenetic characterization of the MIP family of transmembrane channel proteins. *J Membr Biol* **153**:171–180.

Preston GM, Carroll TP, Guggino WB, and Agre P (1992) Appearance of water channels in Xenopus oocytes expressing red cell CHIP28 protein. *Science* **256**:385–387.
Preston GM, Jung JS, Guggino WB, and Agre P (1993) The mercury-sensitive residue at cysteine 189 in the CHIP28 water channel. *J Biol Chem* **268**:17–20.
Reizer J, Reizer A, and Saier MH, Jr (1993) The MIP family of integral membrane channel proteins: sequence comparisons, evolutionary relationships, reconstructed pathway of evolution, and proposed functional differentiation of the two repeated halves of the proteins. *Crit Rev Biochem Mol Biol* **28**:235–257.
Saparov SM, Kozono D, Rothe U, Agre P, and Pohl P (2001) Water and ion permeation of aquaporin-1 in planar lipid bilayers. Major differences in structural determinants and stoichiometry. *J Biol Chem* **276**:31515–31520.
Schwab A, Nechyporuk-Zloy V, Fabian A, and Stock C (2007) Cells move when ions and water flow. *Pflugers Arch* **453**:421–432.
Seeliger D, Zapater C, Krenc D, Haddoub R, Flitsch S, Beitz E, Cerdà J, and de Groot BL (2013) Discovery of novel human aquaporin-1 blockers. *ACS Chem Biol* **8**: 249–256.
Søgaard R and Zeuthen T (2008) Test of blockers of AQP1 water permeability by a high-resolution method: no effects of tetraethylammonium ions or acetazolamide. *Pflugers Arch* **456**:285–292.
Sui H, Han B-G, Lee JK, Walian P, and Jap BK (2001) Structural basis of water-specific transport through the AQP1 water channel. *Nature* **414**:872–878.
Trott O and Olson AJ (2010) AutoDock Vina: improving the speed and accuracy of docking with a new scoring function, efficient optimization, and multithreading. *J Comput Chem* **31**:455–461.
Tsunoda SP, Wiesner B, Lorenz D, Rosenthal W, and Pohl P (2004) Aquaporin-1, nothing but a water channel. *J Biol Chem* **279**:11364–11367.
Yool AJ (2007) Functional domains of aquaporin-1: keys to physiology, and targets for drug discovery. *Curr Pharm Des* **13**:3212–3221.
Yool AJ, Brown EA, and Flynn GA (2010) Roles for novel pharmacological blockers of aquaporins in the treatment of brain oedema and cancer. *Clin Exp Pharmacol Physiol* **37**:403–409.
Yool AJ and Campbell EM (2012) Structure, function and translational relevance of aquaporin dual water and ion channels. *Mol Aspects Med* **33**:553–561.
Yool AJ, Morelle J, Cnops Y, Verbavatz JM, Campbell EM, Beckett EA, Booker GW, Flynn G, and Devuyst O (2013) AqF026 is a pharmacologic agonist of the water channel aquaporin-1. *J Am Soc Nephrol* **24**:1045–1052.
Yool AJ, Stamer WD, and Regan JW (1996) Forskolin stimulation of water and cation permeability in aquaporin 1 water channels. *Science* **273**:1216–1218.
Yoshida T, Hojo S, Sekine S, Sawada S, Okumura T, Nagata T, Shimada Y, and Tsukada K (2013) Expression of aquaporin-1 is a poor prognostic factor for stage II and III colon cancer. *Mol Clin Oncol* **1**:953–958.
Yu J, Yool AJ, Schulten K, and Tajkhorshid E (2006) Mechanism of gating and ion conductivity of a possible tetrameric pore in aquaporin-1. *Structure* **14**: 1411–1423.
Zhang H and Verkman AS (2015) Aquaporin-1 water permeability as a novel determinant of axonal regeneration in dorsal root ganglion neurons. *Exp Neurol* **265**:152–159.
Zhang W, Zitron E, Hömme M, Kihm L, Morath C, Scherer D, Hegge S, Thomas D, Schmitt CP, and Zeier M et al. (2007) Aquaporin-1 channel function is positively regulated by protein kinase C. *J Biol Chem* **282**:20933–20940.

Address correspondence to: Professor Andrea Yool, Medical School South, Level 4, Frome Rd., University of Adelaide, Adelaide SA 5005 Australia. E-mail: andrea.yool@adelaide.edu.au